Geografiska Annaler: Series A, Physical Geography

ISSN: 0435-3676 (Print) 1468-0459 (Online) Journal homepage: http://www.tandfonline.com/loi/tgaa20

Glacier recession in the Altai Mountains of Mongolia in 1990–2016

Caleb G. Pan, Allen Pope, Ulrich Kamp, Avirmed Dashtseren, Michael Walther & Margarita V. Syromyatina

To cite this article: Caleb G. Pan, Allen Pope, Ulrich Kamp, Avirmed Dashtseren, Michael Walther & Margarita V. Syromyatina (2017): Glacier recession in the Altai Mountains of Mongolia in 1990–2016, Geografiska Annaler: Series A, Physical Geography, DOI: 10.1080/04353676.2017.1407560

To link to this article: https://doi.org/10.1080/04353676.2017.1407560

GEOGRAFISKA ANNALER: SERIES A, PHYSICAL GEOGRAPHY, 2017
https://doi.org/10.1080/04353676.2017.1407560

Glacier recession in the Altai Mountains of Mongolia in 1990–2016

Caleb G. Pan[a,b], Allen Pope[c], Ulrich Kamp[d], Avirmed Dashtseren[e], Michael Walther[e] and Margarita V. Syromyatina[f]

[a]W.A. Franke College of Forestry and Conservation, University of Montana, Missoula, MT, USA; [b]Numerical Terradynamic Simulation Group, University of Montana, Missoula, MT, USA; [c]National Snow and Ice Data Center, CIRES, University of Colorado Boulder, Boulder, CO, USA; [d]Department of Natural Sciences, University of Michigan – Dearborn, Dearborn, MI, USA; [e]Mongolian Academy of Sciences, Institute of Geography and Geoecology, Ulaanbaatar, Mongolia; [f]Institute of Earth Sciences, Saint-Petersburg State University, Saint-Petersburg, Russia

ABSTRACT

Relatively little is known about glaciers in the continental climates of North Asia and even less is known about the glaciers of the Mongolian Altai. In an attempt to fill this knowledge gap, we present a new satellite-derived glacier inventory for the Altai Mountains of Mongolia, using the recently launched Landat-8 OLI and Sentinel-2A MSI sensors to monitor glacier change from 1990 to 2016. We examine changes in climatic trends and glacier topomorphological parameters in conjunction with glacier fluctuations to determine governing controls over glacier recession in the Altai Mountains. Our glacier mapping results produced 627 debris-free glaciers with an area of 334.0 ± 42.3 km^2 as of 2016. These data were made available for download through the Global Land Ice Measurements from Space (GLIMS) initiative. A subsample of 206 glaciers that were mapped in 1990, 2000, 2010, and 2016 revealed that from 1990 to 2016, glacier area reduced by 43% at 6.4 ± 0.4 km^2 yr^{-1}. Glacier recession was greatest from 1990 to 2000 at a rate of 10.9 ± 0.8 km^2 yr^{-1}, followed by 2010–2016 at 4.4 ± 0.3 km^2 yr^{-1}. Rates of glacier recession were significantly correlated with intrinsic glacier parameters, including mean, minimum and range elevations, mean slope and aspect. Furthermore, climate records indicated the warmest summer temperatures occurred during periods of high glacier recession.

ARTICLE HISTORY
Received 16 June 2017
Revised 26 September 2017
Accepted 11 October 2017

KEYWORDS
Altai; glaciers; glacier monitoring; Mongolia; climate change

1. Introduction

Glaciers are a keystone feature of terrestrial alpine ecosystems and have become one the best natural proxies for global climate change (Oerlemans 2005; Zemp et al. 2015). The global trend in retreat of glaciers in reaction to global climate change (IPCC, 2013) has implications for both ecological structure and function, and human development. A governor of ecological community composition, glacier sediment transported by melt runoff is an important input for both lentic and lotic aquatic ecosystem biodiversity (Brown et al. 2007; Muhlfeld et al. 2011) and influences limitations on aquatic and terrestrial net primary productivity (Hodson et al. 2008). Glacier melt runoff is also an important water resource for downstream populations at scales ranging between small communities to large metropolitan centers (Bolch et al. 2012; Lutz et al. 2014).

Remotely sensed Earth observation satellites provide one of the most effective means to monitor changes in alpine glaciers, enabling global coverage of multispectral and optical images at moderate spatial resolution, an effective temporal resolution, and at limited costs (Raup et al. 2007; Bhambri

CONTACT Caleb G. Pan caleb.pan@mso.umt.edu W.A. Franke College of Forestry and Conservation, University of Montana, Missoula, MT 59812, USA

and Bolch 2009; Racoviteanu et al. 2009). Many studies have employed satellite images to inventory glaciers at a regional scale to detect changes in glacier area (Tennant et al. 2012; Chand and Sharma 2015; Tielidze 2016). One of the most widely applied sensors in the application of glacier monitoring is the Landsat series beginning in 1972, providing open access to a now 45-year record of global environmental change (Wulder et al. 2012; Pope et al. 2014). Two more recent satellites that provide images useful in glacier monitoring are Landsat 8 Operational Land Imager (OLI) (launched in 2013) (Roy et al. 2014) and Sentinel 2-A MultiSpectral Instrument (MSI) (launched in 2015). These two new sensors are operating at a critical period as Landsat 5 was decommissioned in 2012 and Landsat 7 continues to suffer from a malfunctioning scan-line corrector (Paul et al. 2016).

The glaciers of Mongolia are not well studied and have gained international attention only recently (Ganiushkin et al. 2015; Kamp and Pan 2015; Syromyatina et al. 2015; Zhang et al. 2016; Walther et al. 2017). The Mongolian Altai is located within mid-latitudes of the North Asian landmass. Considering the majority of terrestrial alpine glaciers exist under some form of maritime influence, glaciers of North Asia and Mongolia are some of the few glaciers that exist in a continental climate (Baast 1998). The objectives of this paper are to: (1) map glaciers of the Mongolian Altai using the recently launched Landsat 8 OLI and Sentinel-2A MSI; (2) contribute new data to the previous glacier inventory created by Kamp and Pan (2015) to extend the glacier record for Mongolia and (3) analyze glacier change from 1990 to 2016 to understand the forces that contribute to glacier recession in the Mongolian Altai.

2. Study area

2.1. Regional context

The Altai Mountains form the border between Mongolia and China and trend from the northwest to the southeast for 1200 km before turning east and terminating in the Gobi Desert; they form the most extensive longitudinal mountain range in Central Asia, continuing into Russia to join the Russian Sayan Mountains (Figure 1). There are a number of isolated mountains greater than 4000 m a.s.l. within the Mongolian Altai with the highest elevations in the Tavan Bogd, where Khuiten Peak reaches a maximum elevation of 4374 m a.s.l. (Grunert et al. 2000; Herren et al. 2013; Shinneman et al. 2010).

2.2. Previous studies on glaciers in the Altai Mountains

Long-standing glacier monitoring efforts in the Mongolian Altai do not exist, attributed in large part to the region's sparse population and limited infrastructure, making access to glaciers difficult. In spite of the challenges associated with glaciological methods in the Mongolian Altai, there have been a number of studies that used remotely sensed observations to monitor glacier changes. The majority of these studies focused on the glaciers of Tavan Bogd (Kadota and Gombo 2007; Kadota et al. 2011; Krumwiede et al. 2014), Turgen Mountains (Lehmkuhl 1999; Khrustsky and Golubeva 2008; Kamp et al. 2013), Tsambagarav Uul (Kadota et al. 2011) and Munkh Khairkhan (Krumwiede et al. 2014). A few studies examined glacier area within the entire Mongolian Altai (Selivanov 1972; Devjatkin 1981; Baast 1998; Klinge 2001; Enkhtaivan 2006; Yabouki and Ohata 2009; Kamp and Pan 2015; Nuimura et al. 2015; Earl and Garnder 2016). Within these studies, glacier mapping results were quite sporadic, ranging in total glacier area from 300 km^2 (Devjatkin 1981) to 659 km^2 (Baast 1998). The discrepancy in these results is likely due to: (1) differing source data, (2) differing dates of source data, (3) author groups' definition of 'glacier', (4) glacier mapping methodology and (5) the spatial extent of 'Mongolian Altai'. Only recently has the first satellite-derived systematic mapping and multi-temporal inventory of the Mongolian Altai been completed (Kamp and Pan 2015). To the authors' knowledge, only two of the aforementioned studies mapped debris-covered glaciers in the Mongolian Altai. Aggregating the Russian and Mongolian Altai with the Russian

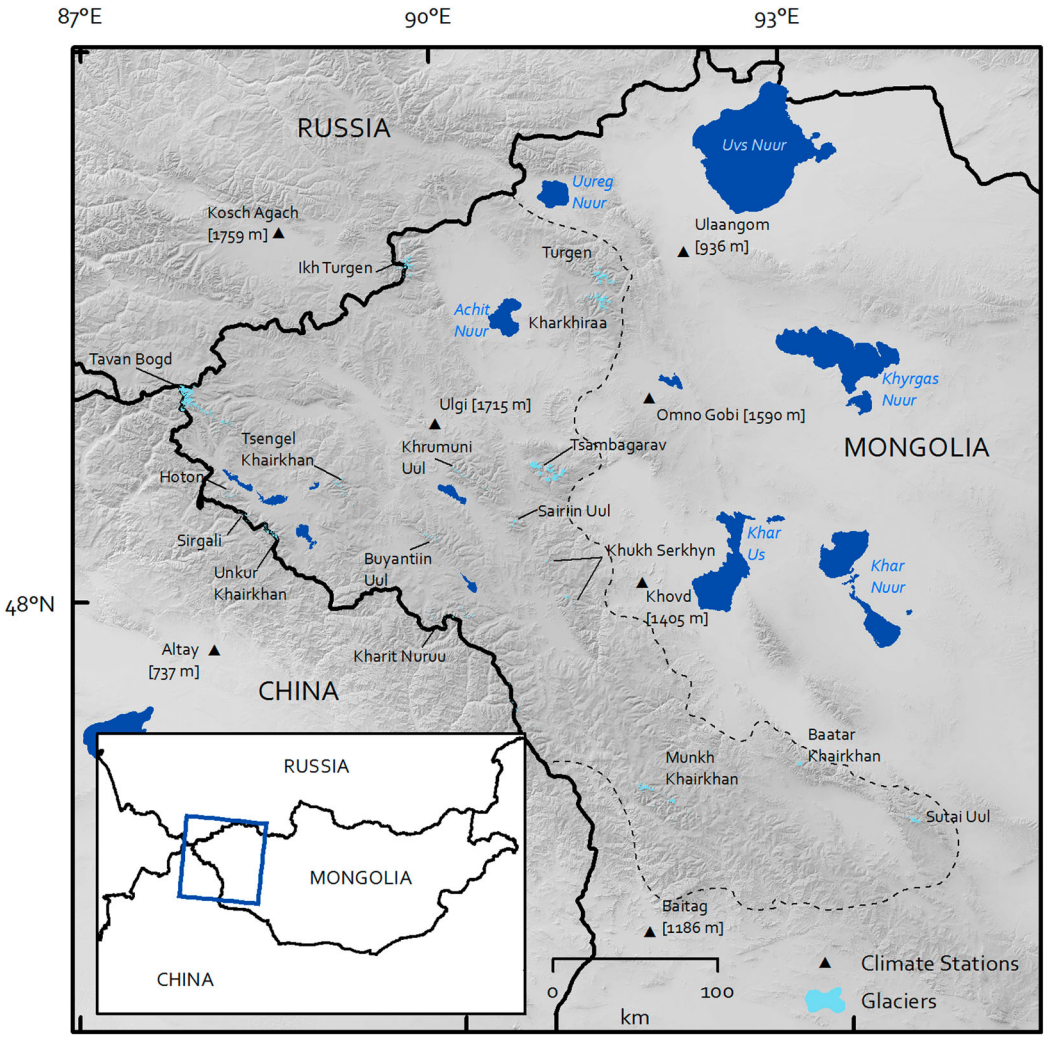

Figure 1. Overview map of the Altai Mountains of Mongolia (defined by the dashed line). Glaciated mountain ranges are identified within the greater Altai complex.

Sayan Mountains, Earl and Garnder (2016) determined that debris-covered glaciers included 42 ± 4 km^2 (3.6%) of the total glacier area. Krumwiede et al. (2014) documented that in Tavan Bogd, the debris-covered area was 3.4 km^2 in 1989 and 2.9 km^2 in 2006.

3. Data and methods

3.1. Satellite data

In this study, we employed Landsat 8 OLI and Sentinel-2A MSI imagery to generate a glacier inventory for the Mongolian Altai for 2016. Images for the new inventory were acquired from the USGS via its Global Visualization viewer (http://glovis.usgs.gov) (Table 1).

Both OLI and MSI possess sensor characteristics that are more advantageous to glacier mapping than earlier Landsat sensors. Improvements to radiometric resolution from 8 bit to 12 bit for OLI and a radiometric resolution of 12 bit for MSI sensors (Winsvold et al. 2016) has proved to be more effective at identifying glaciers within shadows (Kääb et al. 2016). The spatial resolution of

Table 1. Information for the scenes used for the updated glacier inventory, including the classification threshold used for each image (described in Section 3.1).

Satellite	Date	Path/Row or Tile #	Sensor	Threshold
Landsat 8	02 Sep 2014	141/26	OLI	1.21
Landsat 8	24 Aug 2016	140/27	OLI	2.24
Landsat 8	02 Aug 2015	143/26	OLI	1.24
Landsat 8	27 Aug 2015	142/26	OLI	1.50
Sentinel 2A	11 Aug 2016	T46TCS	MSI	3.05
Sentinel 2A	6 Sep 2016	T45UXP	MSI	2.21
Sentinel 2A	6 Sep 2016	T45UXRs	MSI	3.52
Sentinel 2A	6 Sep 2016	T45UWQ	MSI	3.39
Sentinel 2A	13 Sep 2016	T46UCU	MSI	4.70
Sentinel 2A	31 Aug 2016	T46TES	MSI	3.40
Sentinel 2A	13 Sep 2016	T45TYN	MSI	2.06
Sentinel 2A	13 Sep 2016	T45UYP	MSI	3.38

OLI has remained at 30 m, whereas MSI has a spatial resolution of 10 m in the visible and near-infrared (NIR) bands and a 20 m resolution moving into the shortwave infrared (SWIR). Possibly, the most important advantage for glacier mapping facilitated by these two new sensors is an unprecedented temporal coverage. In addition to OLI's image acquisition rate of 16 days, MSI acquires images every 5 days (at the equator). Combined, the synchronous operation of these two sensors greatly improves the annual acquisition of high quality images with limited cloud cover at the end of the ablation season.

We used a 90 m SRTM v4.1 Digital Elevation Model (DEM) downloaded from the CGIAR CSI (www.cgiar-csi.org/data/srtm-90m-digital-elevation-database-v4-1) to characterize our glacier outlines with parameters including: mean, minimum, and elevation ranges, mean slope and mean aspect. The vertical accuracy of the SRTM is spatially variable, with the most significant errors originally existing in areas of steep topography. Voids have been filled with data from various DEM sources, greatly improving the overall quality of the SRTM (Frey and Paul 2012).

3.2. Climate data

The analysis of temperature and precipitation trends was performed on data from six publicly available climate stations within western Mongolia and the Russian Altai; data were acquired from the National Climatic Data Center (https://www.ncdc.noaa.gov/cdo-web/datatools/findstation). These stations ranged in elevation from 936 m a.s.l. in Ulaangom to 1759 m a.s.l. at Kosch Agach (Figure 1 and Table 2). The geographic distribution of these stations is dispersed throughout the margins of the Altai Mountains, with the Ulgi station being the only one within the geographic center. The stations of Ulaangom, Khovd, and Omno Gobi are located at the transition between the desert steppes and the Altai Mountains, while Baitag and Kosch Agach are located at the Altai's southern and northern extents, respectively.

Table 2. Climate stations utilized for climatic trend derivations within the Altai region ('Coverage' is the temporal data availability for a specific period).

Station	Latitude (dd)	Longitude (dd)	Elevation (m a.s.l.)	Period	Coverage (%)
Mongolia					
Baitag	46.12	91.47	1186	1963–2015	65
Khovd	48.02	91.57	1405	1962–2015	96
Omno Gobi	49.02	91.72	1590	1973–2015	62
Ulaangom	49.80	92.08	936	1962–2015	96
Ulgi	48.93	89.93	1715	1962–2015	57
Russia					
Kosch Agach	50.00	88.68	1759	1962–2015	94

Climate data sets were used to examine fluctuations in temperature and precipitation in relation to changes in debris-free glacier area for the Mongolian Altai for the time periods 1990–2016, 1990–2000, 2000–2010 and 2010–2016. Due to the varying degree of elevation ranges, and temporal and spatial coverage, climate data from all six stations were aggregated to create a regional time series of precipitation and temperature trends. We homogenized the aggregated time series by extracting the monthly precipitation and temperature values from each station for a given month and year. The homogenization outputs a monthly mean value from all six stations. Trend coefficients were then extracted from linear regressions for both temperature and precipitation at seasonal and annual rates and for each time period (Bolch 2007; Osmonov et al. 2013; Osipov and Osipova 2014). Furthermore, it must be clarified that a glacier's response to climatic forcing can often manifest as a delayed response (Tennant et al. 2012) that can vary for different glaciers and different regions (Gardent et al. 2014). For this reason, in lieu of presenting climatic data for specific years, we present climatic trends for different periods.

3.3. Mapping debris-free glaciers

Glacier outlines for 1990, 2000 and 2010 were downloaded from the GLIMS database (www.glims.org). This multi-temporal inventory included a debris-free glacier area of 443 km^2 in 1990, 428 km^2 in 2000 and 371 km^2 in 2010 (Kamp and Pan 2015). However, since in their original inventory, Kamp and Pan (2015) were unable to map all glaciers in 1990 owing to significant cloud cover, they corrected the total glacier area for 1990 to 515 km^2 by including glacier outlines from 2000 in the 1990 inventory. As a result, the 1990 total glacier area represents only an estimated minimum that we here use in our glacier change analysis.

To retain glacier inventory integrity, we followed the same mapping approach as Kamp and Pan (2015). In their inventory, a NIR/SWIR band ratio was applied using a threshold of 2 (Bishop et al. 2004; Bhambri and Bolch 2009). Here, we applied the same band ratio using raw digital numbers of NIR and SWIR bands (OLI5/OLI6 and MSI8/MSI11). However, we deviated from the original inventory by qualitatively determining scene-specific image thresholds (Table 1). The threshold was determined visually with the criteria to be as low as possible to include slightly dirty ice margins (Paul et al. 2013). The average threshold was 1.5 for OLI images and 3.2 for MSI images. A 3×3 median filter was applied to band ratio thresholding results to remove misclassified isolated pixels before being converted to vector polygons. The polygons were aggregated, and a size threshold of 0.01 km^2 was applied. The glacier polygons were intersected with DEM-derived ice divides to segregate the entire debris-free glacier cover into individual glaciers (Bolch et al. 2010). After intersecting, the debris-free glaciers were manually edited to merge sliver polygons to larger adjacent glacier entities (Racoviteanu et al. 2009; Frey et al. 2012). Finally, we assigned each glacier outline either a GLIMSID from the previous inventory or a new GLIMSID (Raup et al. 2007).

3.4. Uncertainty and error

Uncertainty and error in the mapping of debris-free ice can be manifested through a number of steps and processes. Addressing potential sources of uncertainty and error is critical as they can propagate through sequential steps and change detection analysis (Paul et al. 2013; Racoviteanu et al. 2015). In our update of the glacier inventory, uncertainty and errors can potentially originate from: (1) the use of images with varying spatial resolutions; (2) image threshold selection; (3) the misclassification of snowpack as ice; and (4) accuracy of the ice divides derived (Racoviteanu et al. 2009; Nuth et al. 2013).

We represented error as the residual error between the modeled and observed, which takes the following form:

$$E = \sqrt{E_i - \hat{E}_i^2}, \tag{1}$$

Table 3. Mapping results from the 1990–2010 glacier inventory after Kamp and Pan (2015) and for the new 2016 glacier inventory.

	Year/period	Total	Subsample (206)
Area (km^2)	1990	443.1 ± 54.9 [690] 515[a]	391.38 ± 41.7
	2000	428.6 ± 59 [716]	281.88 ± 31.8
	2010	371.1 ± 54.4 [671]	250.1 ± 36.7
	2016	334 ± 44.4 [627]	223.9 ± 29.8
Absolute change (km^2)	1990–2016	181.0 ± 8.4	167.48 ± 11.36
	1990–2000	86.4 ± 3.3	109.5 ± 7.4
	2000–2010	57.5 ± 2.2	31.78 ± 2.2
	2010–2016	66.5 ± 2.7	26.2 ± 1.8
Rate of change ($km^2\ yr^{-1}$)	1990–2016	7.0 ± 0.3	6.4 ± 0.4
	1990–2000	8.6 ± 0.3	10.9 ± 0.8
	2000–2010	5.8 ± 0.2	3.2 ± 0.2
	2010–2016	11.1 ± 0.4	4.4 ± 0.3

Note: Area in km^2; bracketed numbers indicate the number of glaciers. See Section 3.3 of the text.
[a]This is the corrected assumed total glacier area that makes up for missing satellite imagery. See the text for explanations.

where E_i is the area of the glacier polygon and $\hat{E}_i$ is the glacier area determined by the pixel count multiplied by the image resolution. $\hat{E}_i$ is derived from a Perkal's epsilon band around each glacier outline and is buffered by the image resolution to represent a potential error within one pixel (Racoviteanu et al. 2009, 2015; Bolch et al. 2010). Analysis of glacier uncertainty has been documented to be <5% (Paul et al. 2013; Lynch et al. 2016). Our representation of uncertainty can be seen as a conservative assessment with values of 12.4% for 1990, 13.8% for 2000, 14.7% for 2010 and 12.6% for 2016.

4. Results

4.1. Updated glacier inventory

Our updated multi-temporal inventory resulted in 627 debris-free glaciers contributing to a total surface area of 334.0 ± 42.3 km^2 in 2016 (Table 3). In 2016, almost 60% of the glaciers were smaller than 0.125 km^2, and less than 2% were greater than 5.6 km^2; the mean glacier area was 0.53 km^2, the largest glacier area – that of the combined Potanin and Alexandra glaciers – was at 35.5 km^2. The minimum glacier elevation was 2708 m a.s.l., and the mean glacier elevation was 3449 m a.s.l. (Table 4).

4.2. Glacial changes

4.2.1. Glacier area changes

From 1990 to 2016, the debris-free area of the 627 glaciers decreased by 181.0 ± 8.4 km^2 (35%); it decreased by 86.4 ± 3.3 km^2 (16.9%) from 1990 to 2000, 57.5 ± 2.2 km^2 (13.3%) from 2000 to 2010, and 66.5 ± 2.7 km^2 (18.1%) from 2010 to 2016. From 1990 to 2016, the rate of recession was 7.0 ± 0.3 $km^2\ yr^{-1}$, with the highest rate of 11.1 ± 0.4 $km^2\ yr^{-1}$ for 2010–2016, followed by 8.6 ± 0.3 $km^2\ yr^{-1}$ for 1990–2000 and 5.8 ± 0.2 $km^2\ yr^{-1}$ for 2000–2010.

From henceforth, areal and topomorphological changes will be performed on a subsample of 206 glaciers. To be included in this subsample, a glacier was required to have been mapped and possess an area greater than 0.01 km^2 during all four time periods. It should also be noted that, if a glacier

Table 4. Temporal changes of parameters of glaciers in the Mongolian Altai using the 206 subsampled glaciers.

Glacier parameter	1990	2000	2010	2016
Mean elevation (m a.s.l.)	3437	3442	3450	3470
Minimum elevation (m a.s.l.)	2586	2610	2704	2709
Elevation range (m)	412	353	318	303
Mean slope (°)	20	20	20	20
Mean aspect (°)	148	147	144	143

disintegrated into multiple parts, only the part that contained the GLIMSID remained within the subsample of 206. Glacier area in our subsample decreased by 43% from 1990 to 2016, 28% from 1990 to 2000, 11% from 2000 to 2010 and 10% from 2010 to 2016. Furthermore, the rates of glacier recession were 6.4 ± 0.4 km^2 yr^{-1} for 1990–2016, 10.9 ± 0.8 km^2 yr^{-1} for 1990–2000, 3.2 ± 0.2 km^2 yr^{-1} for 2000–2010 and 4.4 ± 0.3 km^2 yr^{-1} for 2010–2016.

Our sample of 206 glaciers showed that both absolute and relative changes in debris-free glacier area indicated that larger glaciers (>0.86 km^2) had the greatest change in area (Figure 2(a)). From 1990 to 2000, glaciers expressed the greatest change in area for all class sizes (Figure 2(b)). During this time, small glaciers (<0.125 km^2) expressed the greatest loss in relative area, although mapping results indicate greater temporal variability within this class size, as positive relative area values can be observed during other time periods. The highest absolute rates of recession during 1990–2016 and 1990–2000 can be partially attributed to the disintegration of large glaciers into smaller glaciers.

4.2.2. Changes in glacier topomorphology

Changes in glacier topomorphologic characteristics indicate significant glacier recession (Table 4). From 1990 to 2016, the mean elevation of debris-free glaciers increased by 33 m, with the largest increase of 20 m during 2010–2016. The minimum glacier elevation increased by 123 m from 1990 to 2016, with the largest increase of 94 m during 2000–2010 and only 5 m during 2010–2016. The mean elevation range decreased by 109 m during 1990–2016, with the largest decrease of 59 m during 1990–2000 and only 15 m during 2010–2016. The changes in minimum elevation and mean elevation range indicate that debris-free glaciers experienced the highest rates of recession from 1990 to 2000. Glacier hypsometries indicate that the debris-free glacier surface area below 3500 m decreased by 20.2% and by 15.5% above 3500 m (Figure 3).

From 1990 to 2016, the mean glacier slope more or less stagnated – it changed only from 20.4° to 20.3°. However, for smaller glaciers (<0.86 km^2) the mean slope decreased by 1.4° from 23.0° to 21.6°, while for larger glaciers (>0.86 km^2) it decreased by 2.2° from 17.6° to 15.4°.

In 2016, debris-free glaciers with an eastern aspect (36.7%) constituted the largest surface area, followed by northeast (33.2%) and southeast (16.5%) aspects. Debris-free glaciers with a northeast, northwest or northern aspect – aspects that in the northern hemisphere favor glacier health – had a share of 26% in 1990, 41% in 2000, 36% in 2010 and 39% in 2016 of the total glacier area. However, when looking at the total number of glaciers, these three aspects constituted 52% in 1990, 59% in 2000, 62% in 2010 and 62% in 2016, suggesting that small glaciers are mainly situated in northern aspects (Figure 4).

The rate of glacier change was negatively correlated with glacier area, mean elevation and elevation range. Positive correlations were found between mean aspect, mean slope and minimum elevation. Regressions performed on the rates of glacier change for 1990–2016 for all parameters were significant at the 99% confidence interval ($p < .01$). In an attempt to identify fluctuations in controls of glacier recession, regressions were performed for rates of glacier change during 1990–2000, 2000–2010 and 2010–2016. Significance and correlations weakened for all three sub-periods relative to entire period of 1990–2016. Yet, glacier area and elevation range remained significant at the 99% confidence interval ($p < .01$) for all four periods. Mean elevation and mean aspect were significant at the 95% confidence ($p < .05$) interval. Minimum elevation was significant for all periods at the 90% confidence interval ($p < .1$). For the time periods of 2000–2010 and 2010–2016, mean slope became an insignificant control of the rate of glacier change at the 90% confidence interval ($p < .1$).

4.2.3. Qualitative analysis of glacier change

Although this study did not attempt to apply a DEM-differencing approach to quantify glacier thinning (Bolch et al. 2008), the downwasting of debris-free glaciers is evident through qualitative visual inspection. Throughout all subregions of the Altai Mountains, many larger glaciers have

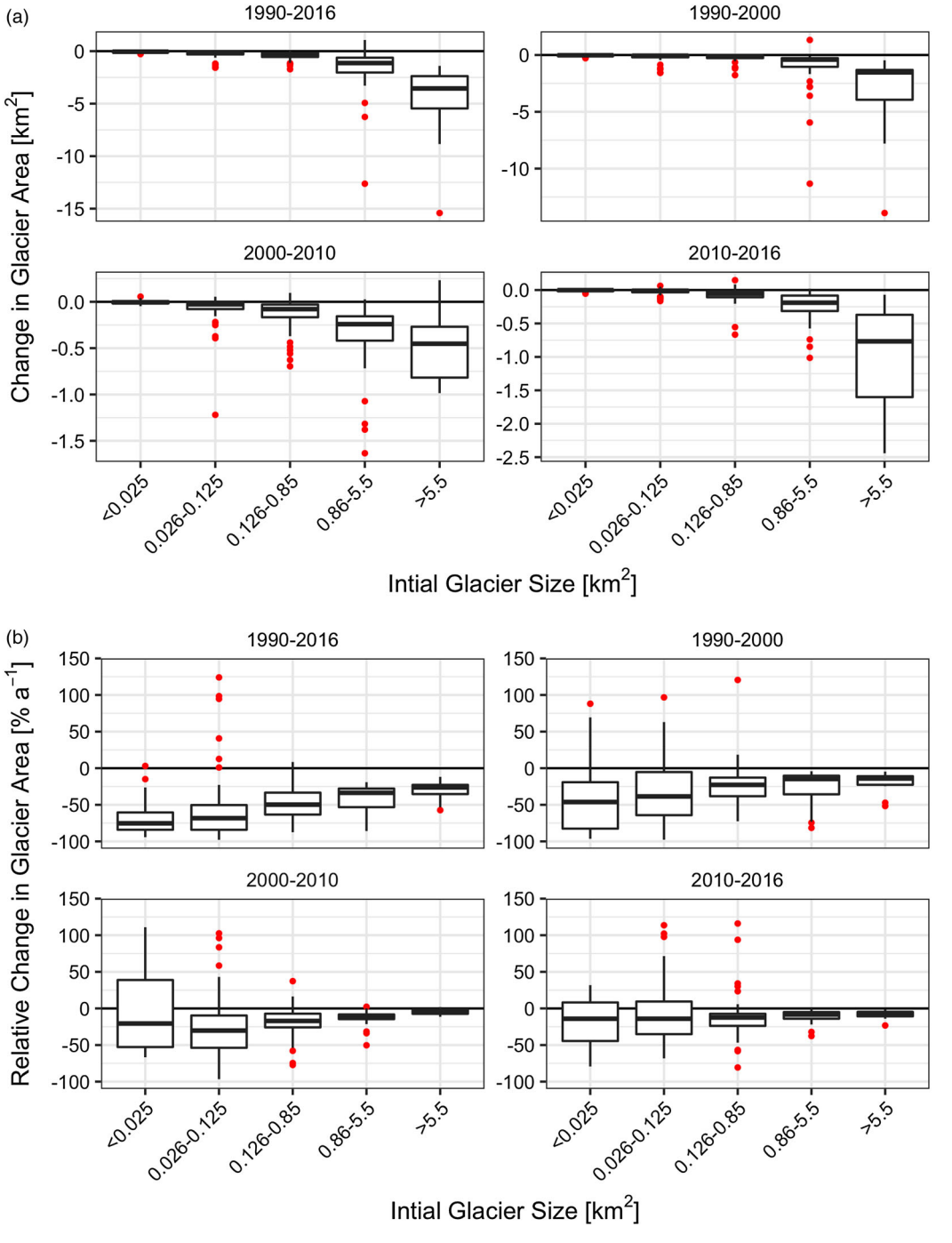

Figure 2. (a) Boxplots of absolute change in glacier area by class size in the Mongolian Altai. Red dots indicate outliers. (b) Boxplots of relative change in glacier area by class size in the Mongolian Altai. Red dots indicate outliers.

disintegrated into smaller glaciers and most notably, this study presents the first evidence of the separation of the Altai's two largest glaciers, Potanin and Alexandra in the Northwest Interior (Figure 5). Downwasting is also documented through the development of proglacial lakes and increased exposure of nunataks as a result of glacier recession (Paul et al. 2007).

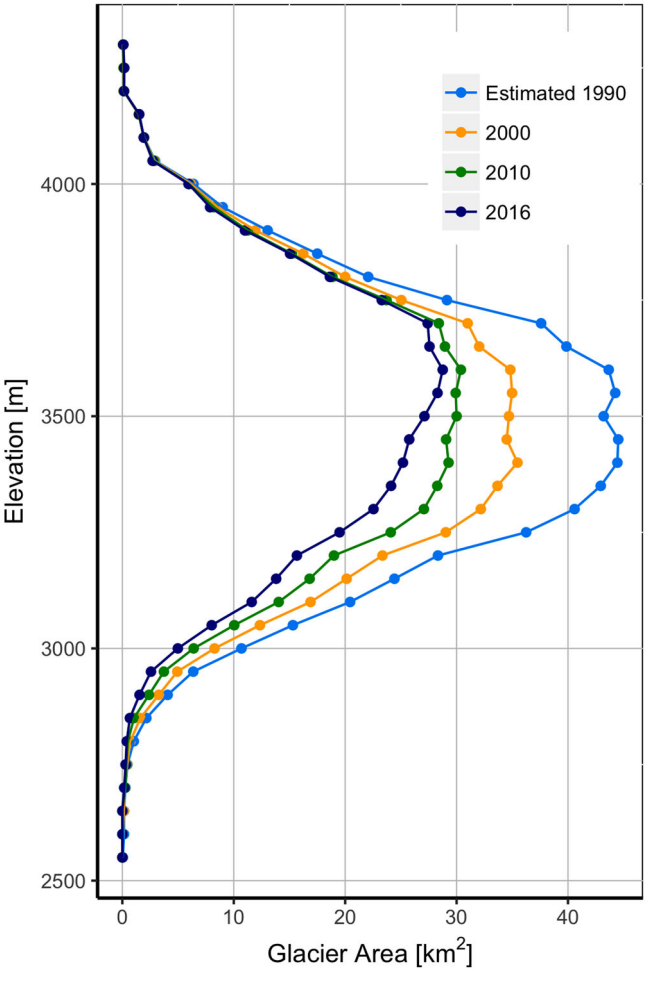

Figure 3. Hypsometries of glaciers in the Mongolian Altai, including debris-covered glaciers.

4.3. Current climatic trends

Trend coefficients indicated an increase in mean annual air temperature (MAAT) of 0.007°C yr^{-1} from 1962 to 2015, with an amplified increase of 0.19°C yr^{-1} from 1989 to 2015 (Figure 6 and Table 5). Seasonally and temporally aggregated air temperature trends indicated fluctuating positive and negative trends. From 1989 to 2015, the period of interest for our glacier monitoring, spring and summer seasons observed negative trends only during 2000–2010 (Figure 7). Furthermore, the summer months observed the highest annual increase in air temperature at 0.12°C yr^{-1} during 1989–2000, followed by 2010–2015 at 0.07°C yr^{-1}.

From 1962 to 2015, regional precipitation trends had higher variability relative to temperature trends (Figure 8 and Table 6). Yet, there was an observable increase in annual precipitation of 0.28 mm yr^{-1} from 1962 to 2015, and an amplified trend of 0.81 mm yr^{-1} from 1989 to 2015. However, within these overall increases in mean annual precipitation trends, there were distinct seasonal and temporal characteristics (Figure 9). The summer months during all time periods observed negative trends with highest trends occurring during 2010–2015 followed by 1989–2000. During the winter, spring and fall seasons, positive trends were observed for the most part during all time periods.

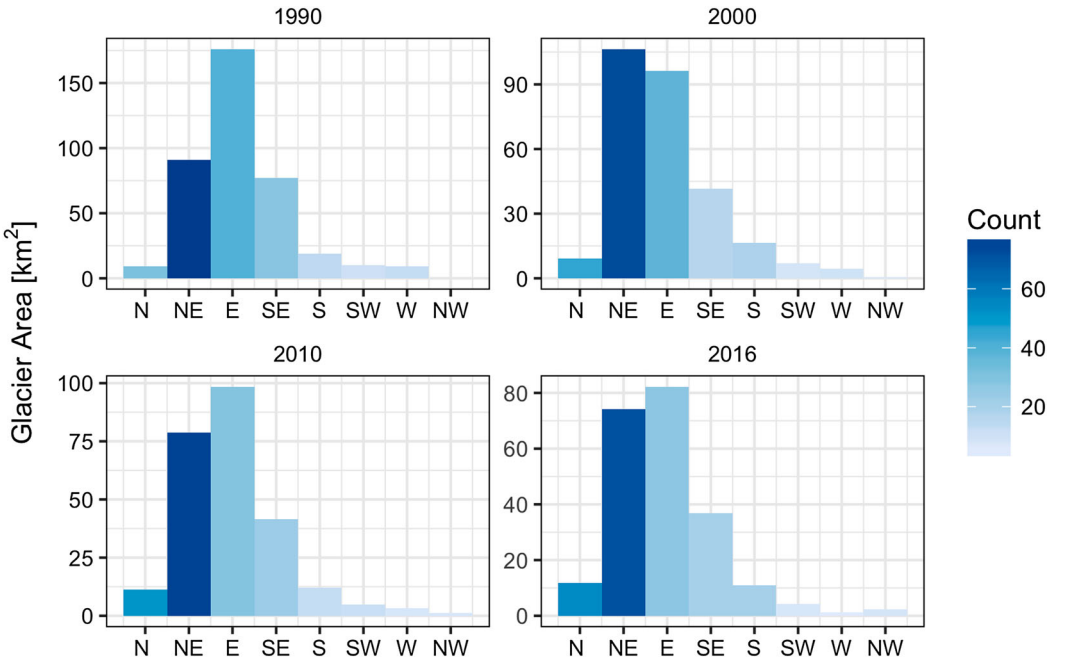

Figure 4. Distribution of area and number of glaciers by aspect in the Mongolian Altai.

5. Discussion

5.1. Comparison between different inventories

A comparison of our inventory results with those from Kamp and Pan (2015) proves challenging. As explained earlier, Kamp and Pan (2015) could not map all glaciers for 1990 owing to significant cloud cover in some satellite scenes and, hence, estimated and then added the missing glacier area to the mapped one. They put the decrease in glacier area in the Mongolian Altai at 28% between 1990 and 2010. By extending the study period to 1990–2016, we found a decrease in area of 35% for all 627 glaciers, and of 43% for only the 206 glaciers for which mapping results are available for all four years of 1990, 2000, 2010 and 2016. However, both cases document a continuation of the glacier recession after 2010.

The strong rates of glacier recession in the Mongolian Altai are above those documented in glacier inventories for regions with more maritime climates. For example, several authors reported a decrease in glacier area of 19% from 1985 to 2006/2009 in the French Alps (Gardent et al. 2014), 25% from 1985 to 2011 in Northern Patagonia (Paul and Mölg 2014) and 11% from 1985 to 2005 in western Canada (Bolch et al. 2010). More locally relevant, observations in the Chuya Ridge and Russian Altai indicated a glacier area reduction of 19.7% from 1952 to 2004 (Khromova et al. 2010; Shahgedanova et al. 2010). Other glacier inventories within the region are in strong agreement with our results for the Mongolian Altai. For example, Stokes et al. (2013) documented a decrease in glacier area of around 40% from 1995 to 2011 in the Kodar Mountains of east-central Siberia.

Additionally, our results show that glaciers in the Altai Mountains decreased by 29% from 2000 to 2016, which is similar to the reduction of 24% from 2000 to 2014 for the Kamchatka Penninusla (Lynch et al. 2016). In the east Sayan, Baikalsky and Kodar Mountains of southeast Siberia, Osipov and Osipova (2014) found a reduction in glacier area of 27% from 2001/02 to 2006/11.

Notably, of the few glacier inventories within extreme continental climates (Surazakov et al. 2007; Stokes et al. 2013; Osipov and Osipova 2014) and milder continental climates (Lynch et al. 2016),

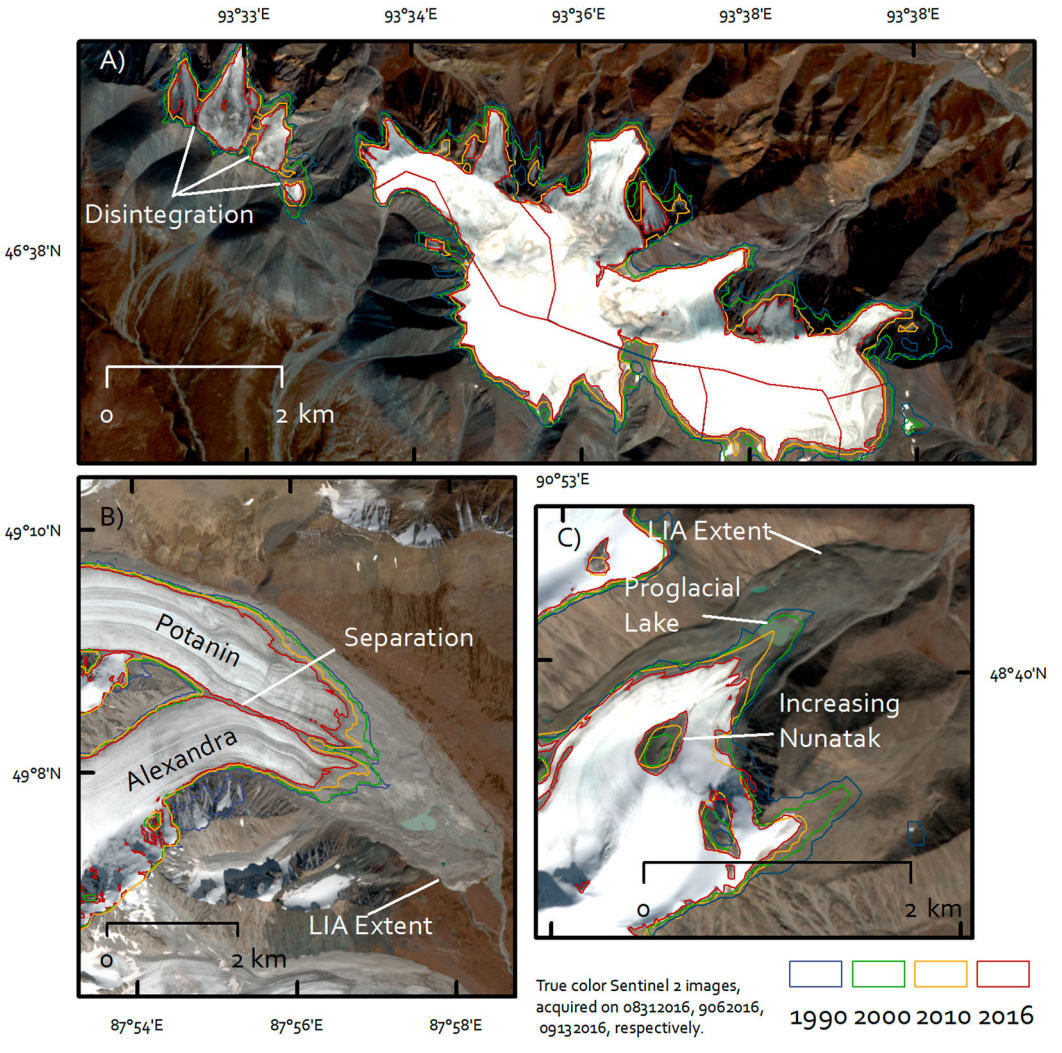

Figure 5. Examples of glacier change in the Mongolian Altai. (A) Sutai Uul in the Southern Altai exhibits the disintegration of a larger glacier into smaller glaciers, a common trend throughout the region. (B) The tongues of Mongolia's two largest glaciers, Potanin and Alexandra, began separating from each other for the first time in 2016. The distance of Alexandra to the end of the Little Ice Age (LIA) extent was about 2.6 km. From 1990 to 2016, the terminus of (originally combined) Potanin/Alexandra glacier retreated by 597 m. (C) Tsambagarav Uul in the Central Altai demonstrates the development of a proglacial lake between 1990 and 2000, and a 'growing' nunatak in the center of the lower portion of the glacier. The distance between the LIA extent and the 2016 termini was 1.6 km. Between 1990 and 2016, the terminus retreated by 636 m.

changes in glacier area are in the best agreement with the results for the Altai Mountains. The comparison of global and regional glacier inventories suggests that probably in recent decades continental alpine glaciers have observed a greater reduction in areal extent in comparison to maritime alpine glaciers. However, a more exhaustive review of the literature will be required to draw strong conclusions.

5.2. Topomorphological characteristics and glacier recession

Despite the correlation and significance determined by regression analysis between glacier rates of change and topomorphological characteristics, it is difficult to determine the degree of influence of

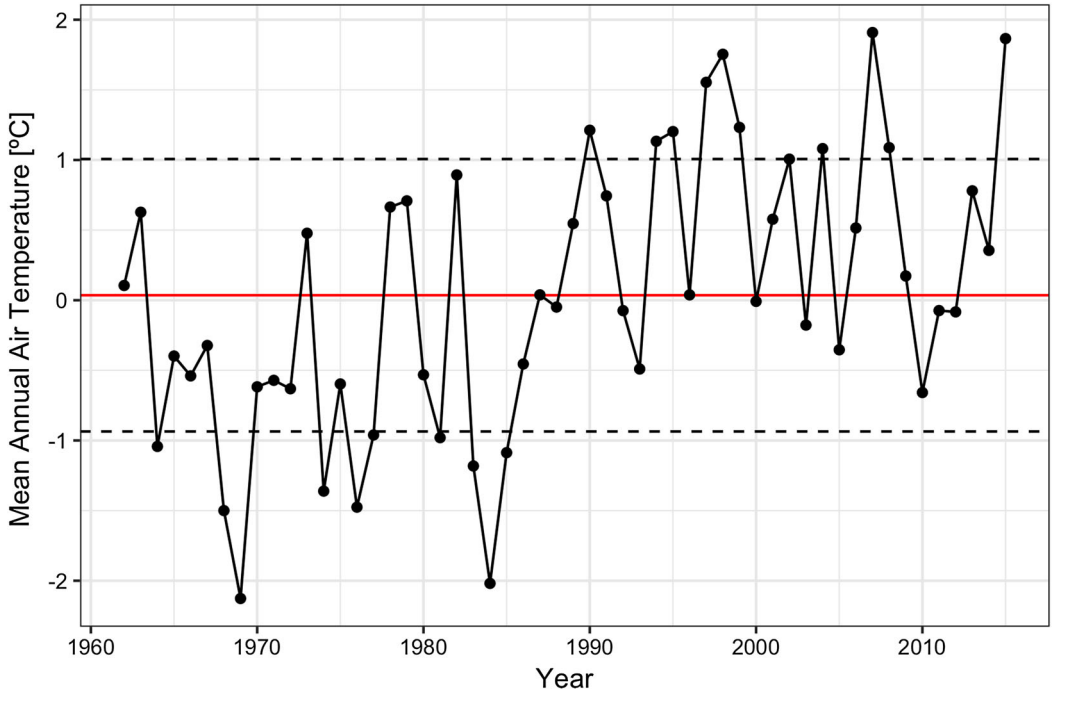

Figure 6. Mean annual air temperature from 1962 to 2015 in the Mongolian Altai. Red line indicates the mean MAAT. Dashed black lines indicate one standard deviation.

topomorphological glacier characteristics on their recession. A glacier's elevation is not entirely independent of the glacier area largely because the elevation is an intrinsic characteristic of a glacier and results in high correlations between changes in mean and elevation ranges and the rates of glacier recession. In other words, it is difficult to determine the influence of topomorphological characteristics on glacier recession because mean elevation and elevation ranges are largely determined by a glacier's area. Hence, any changes in glacier area will be proportionally reflected in changes of mean elevation and elevation ranges. However, a glacier's minimum elevation is not a derivative of its length or a proxy of its size, providing credence to minimum elevation as being one of the more independent and appropriate topomorphological glacier parameters. We identified accelerated rates of glacier recession in glaciers that possess a minimum elevation above 3500 m a.s.l ($p < .001$) relative to rates of recession below 3500 m a.s.l ($p < .001$). The accelerated increase in glacier minimum elevation at higher elevations may be an indicator of glaciers trending towards slopes that are less shaded and are more exposed to solar radiation. Osipov and Osipova (2014) found results contrary to the results on minimum glacier elevation presented here, and other regional studies found no statistical significance between area loss and minimum elevation (Stokes et al. 2013; Lynch et al. 2016).

Table 5. Trend coefficients (°C yr^{-1}) of temperature derived as seasonal aggregate means from six climate stations within the Mongolian Altai.

Period	Winter	Spring	Summer	Fall	Annual
1962–2015	0.041	0.028	0.019	0.041	0.032
1962–1989	0.052	−0.007	0.000	0.065	0.019
1989–2015	−0.108	0.045	0.035	−0.046	−0.007
1989–2000	0.028	0.137	0.118	−0.152	0.038
2000–2010	−0.183	−0.061	−0.015	0.232	−0.009
2010–2015	0.183	0.196	0.069	−0.078	0.422

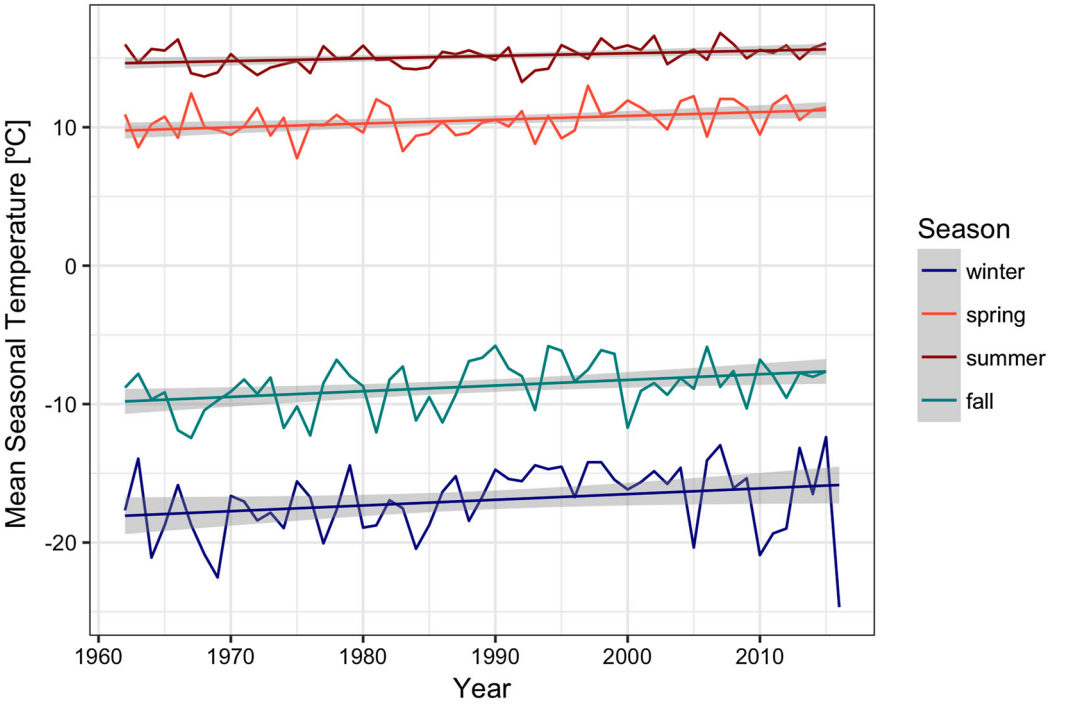

Figure 7. Seasonal temperature trends (including the standard deviation) between 1962 and 2015, derived from six climate stations within the Altai Mountains. Increasing temperature trends can be observed for all seasons.

Tsutomu and Gombo (2007) used the term 'flat-top' to describe many of the glaciers throughout the Altai Mountains. This terminology is used to qualitatively define the topomorphological context of Altai glaciers, in that many of the glaciated mountain peaks are quite homogenous with shallower slopes. The homogeneity reduces the topographic complexity and increases the exposure of glaciers to solar radiation at higher elevations. We can interpret the decrease in mean slopes for glaciers throughout the Altai Mountains as a consequence of glaciers receding from lower elevations to the more exposed 'flat-top' regions of these mountain tops. This possibility is in line with the accelerated recession at higher elevations determined by changes in minimum elevation as the glaciers become more exposed to solar radiation (Tennant et al. 2012; Osipov and Osipova 2014).

The northern aspect was the only aspect that consistently observed an increase in number of glaciers and consequently an increase in area for all years. As glaciers with initial aspects of northwest, northeast or east begin to recede, they possess the propensity to recede in a fashion that evolves their aspect towards the north (DeBeer and Sharp 2007), thus increasing the number of glaciers with a northerly aspect. Considering the minor increase in area relative to the increase in number for glaciers with a north aspect, we conclude that these glaciers are smaller and protected by steeper slopes. Yet, even though small glaciers are transitioning into northern aspects, small glaciers still expressed higher relative rates of recession, and as a consequence we must consider aspect to possess a subdued role in the modulation of glacier recession (Granshaw and Fountain 2006).

5.3. Regional climatic trends

Regional climatic trends throughout the mountain environments of western Mongolia and southern Siberia indicate consistent warming trends. From two climate stations in southeastern Siberia, Osipov and Osipova (2014) found a general trend of summer temperature increase at a rate of 1.7°C and 2.6°C, respectively, for 1970–2010. Within the adjacent Kodar Mountains, the mean summer

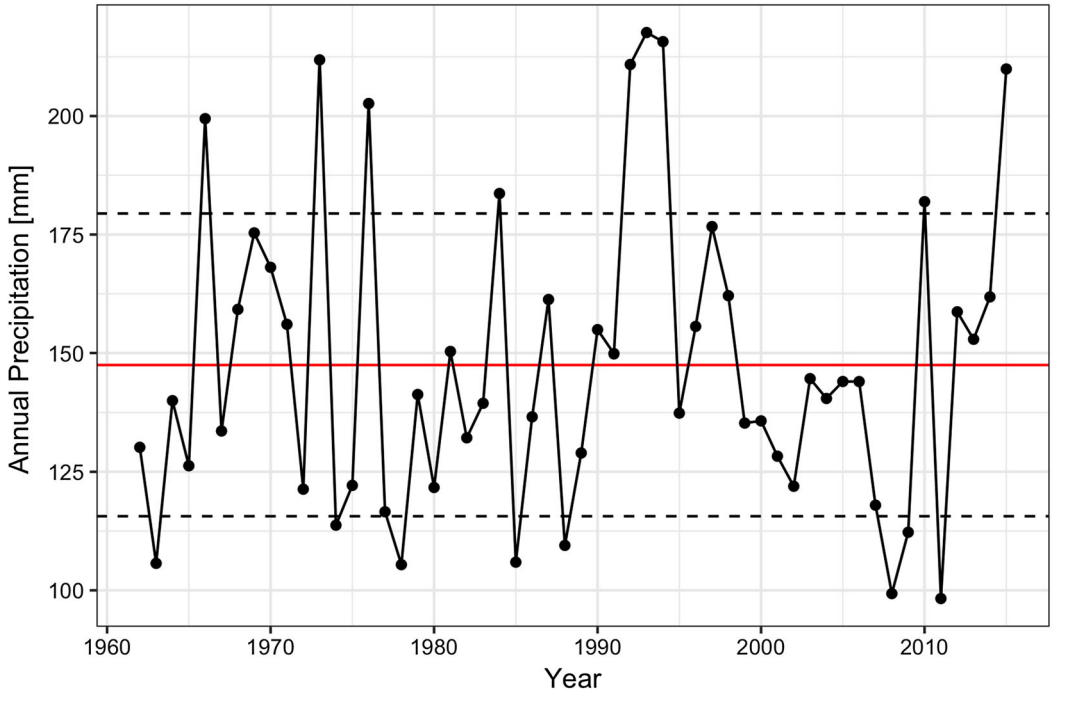

Figure 8. Annual precipitation from 1962 to 2015. Red line indicates the mean annual precipitation. Dashed black lines indicate one standard deviation.

temperature was 13.9°C for 1960–1995; however, in more recent decades, the mean summer temperatures increased by 1.1°C to 15°C for 1995–2010 (Stokes et al. 2013). In the more local Russian Altai, Shahgedanova et al. (2010) observed an increase in summer temperatures by 1.26°C from 1950 to 2004, and by 1.9°C from 1985 to 2004. Interestingly, from 1951 to 2000, mean summer temperatures in the Aktru Basin increased by 1.03°C below 2500 m a.s.l. and by 0.83°C above 2500 m a.s.l., which is attributed to increased summer precipitation at higher elevations (Surazakov et al. 2007). For the Altai Mountains, we observed an increase in summer temperatures of 1°C from 1962 to 2015. Indeed, our results of climatic trends also demonstrate accelerated rates of summer temperature increase in recent decades and are in agreement with the rates of glacier recession in the Altai Mountains.

Given that the climate stations are at lower elevations than the glaciers, it is difficult to assess the interaction between precipitation trends and glacier recession. Precipitation during the accumulation (October–March) season has been historically limited by the Siberian High. However, the Siberian High has been undergoing considerable weakening, allowing greater amounts of precipitation during the accumulation season (Shinneman et al. 2010). Our results indicate positive trends in winter precipitation (1962–2015, 1989–2015), though these trends are at low magnitude despite the weakening

Table 6. Trend coefficients (mm yr^{-1}) of precipitation derived as seasonal aggregate means from within six climate stations with the Mongolian Altai.

Period	Winter	Spring	Summer	Fall	Annual
1962–2015	0.010	0.133	−0.350	0.239	0.063
1962–1989	−0.177	0.263	−0.499	0.048	−0.365
1989–2015	0.284	0.335	−2.085	0.381	−0.931
1989–2000	0.236	0.074	−3.110	1.220	−1.581
2000–2010	1.388	−0.787	−0.174	0.018	0.445
2010–2015	−0.310	6.346	−5.575	5.285	9.283

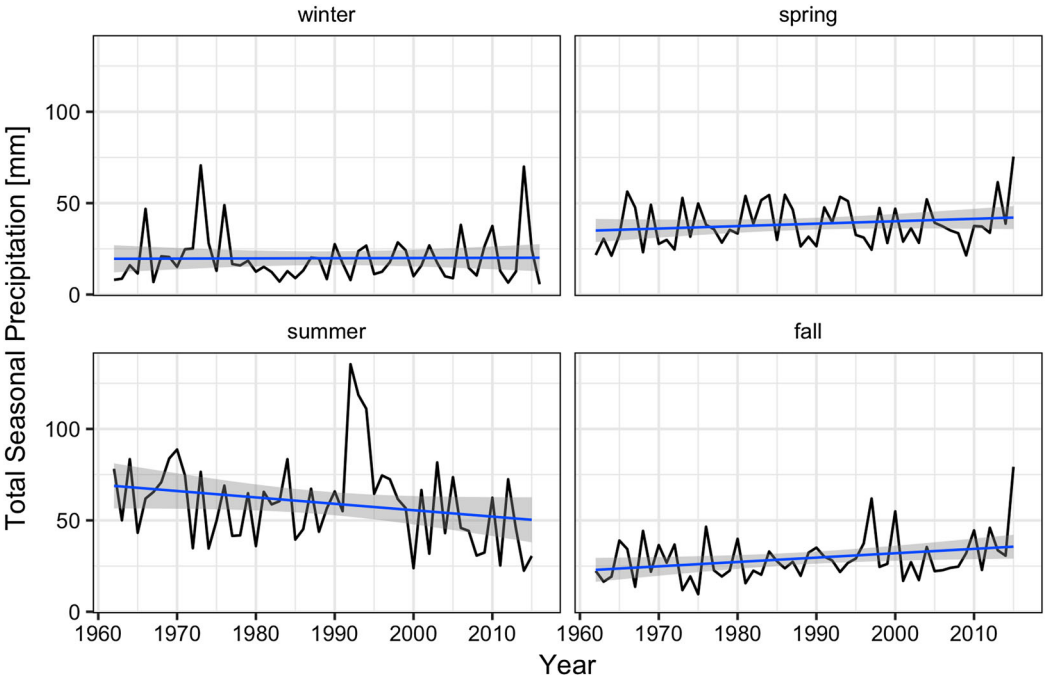

Figure 9. Seasonal precipitation trends (including the standard deviation) between 1962 and 2015, derived from six climate stations within the Altai Mountains. Decreasing summer precipitation can be observed while increasing precipitation trends are occurring in the fall and spring.

of the Siberian High. It could be possible that its weakening is expressed by increased spring precipitation, which could be a result of the Siberian High Pressure being replaced by the Asiatic Low at an earlier time during the year. It is difficult to define how these changes in precipitation are influencing glacier recession in the Altai Mountains over time, particularly because it is unclear if the precipitation is falling as snow or rain. We can hypothesize that decreasing summertime precipitation can be a representative proxy for increased number of cloud-free days, which in turn enhances the amount of incoming solar radiation. However, the dominant surface energy balance of Altai glaciers is unknown (Francou et al. 2003). While the increasing precipitation during the spring and fall seasons can be either rain or snow, with enhanced rates of increased temperature during these seasons, it is also possible that the glaciers in the Altai Mountains are receiving more rain in lieu of snow, which can accelerate the ablation processes (Osipov and Osipova 2014).

Summary

We here continued our monitoring of glaciers in the Mongolian Altai and extended the period of the older inventory that covered the period from 1990 to 2010 (Kamp and Pan 2015) to now 2016 by using Landsat 8 OLI and Sentinel 2A-MSI. Our new glacier outlines for 2016 – like the ones for 1990, 2000 and 2010 from the first inventorying study – can be accessed from the GLIMS database website free of charge (Kargel et al. 2005). The new inventory consists of 627 debris-free glaciers covering an area of 334.0 ± 42.3 km^2 as of 2016. Our analysis of glacier change on a subset of 206 glaciers showed a decrease in debris-free glacier area of 43% at a rate of 6.4 ± 0.4 $km^2\ yr^{-1}$ from 1990 to 2016. The highest rates of recession occurred during 1990–2000 at 10.9 ± 0.8 $km^2\ yr^{-1}$. While some studies from other mountain ranges in the region present recession rates that are similar to the relatively strong recession of glaciers in the Mongolian Altai, others found much slower recessions. However, it seems that glaciers in the extreme continental Mongolian Altai are receding at higher rates than in

many other mountain ranges worldwide. Mean summer temperatures are likely the primary driver of this accelerated glacier recession in the Altai Mountains, as there has been a measured increase of 1°C from 1962 to 2015 and an enhanced increase since 1990. The greatest increase in summer temperature correlates well to accelerated periods of glacier recession, particularly for 1990–2000 and 2010–2016. However, the topomorphological characteristics of debris-free glaciers also express certain controls on glacier recession.

Acknowledgements

The authors would also like to thank two anonymous reviewers for their constructive and thoughtful comments. C. Pan, A. Dashtseren and M. Walther carried out fieldwork; C. Pan, A. Pope, A. Dashtseren and M. Syromyatina analyzed the data; C. Pan designed the study and wrote the manuscript with U. Kamp and A. Pope.

Disclosure statement

No potential conflict of interest was reported by the authors.

Funding

C. Pan was supported by the Montana Space Grant Consortium (MSGC) Student Research Fellowship, American Center for Mongolian Studies (ACMS) Summer Research Fellowship, U.S. Department of State's Fulbright Program, University of Montana Office of Research and Creative Scholarship, and the U.S. Embassy – Ulaanbaatar, Mongolia Grants Program. A. Pope was supported by USGS contract G12PC00066.

Notes on contributors

Caleb G. Pan is a Systems Ecology PhD student working in the Numerical Terradynamic Simulation Group at the University of Montana, with a research focus in the application of remote sensing to understand cryospheric processes.

Allen Pope is a research scientist at the National Snow and Ice Data Center; his area of research is remote sensing of the global cryosphere, in particular with multispectral satellite data.

Ulrich Kamp is a Professor in Geology and Environmental Science at the University of Michigan—Dearborn. He has research interests in the cryosphere, environmental change, geomorphology, mountain geography, and natural hazards.

Avirmed Dashtseren is the head of the Division of Permafrost at the Institute of Geography and Geoecology in the Mongolian Academy of Sciences. His main scientific interests are permafrost, seasonally frozen ground, glaciers, and their interaction with climate and ecosystems.

Michael Walther is currently a Senior Scientist at the Institute of Geography and Geoecology in the Mongolian Academy of Sciences. His fields of research focus on climate change, landscape development and Natural Resource Management in Central Asia.

Margarita Syromyatina is a research fellow in the Institute of Earth Sciences at Saint-Petersburg University, Russia. Her research interests are in mountain geosystems, mountain hydrology, climate change, and mountain land use.

References

Baast P. 1998. Modern glaciers of Mongolia. Unpublished report, 162. Ulaanbaatar: Institute of Meteorology and Hydrology (In Russian).

Bhambri R, Bolch T. 2009. Glacier mapping : a review with special reference to the Indian Himalayas. *Prog Phys Geogr*. 33:672–704. doi:10.1177/0309133309348112.

Bishop MP, Olsenholler JA, Shroder JF, Barry RG, Raup H, Bush ABG, Copland L, Dwyer JL, Fountain AG, Haeberli W, et al. 2004. Global land ice measurements from space (GLIMS): remote sensing and GIS investigations of the Earth' s cryosphere global land ice measurements from space (GLIMS): remote sensing and GIS investigations of the Earth's cryosphere. *Geocarto Int*. 19:57–84.

Bolch T. 2007. Climate change and glacier retreat in northern Tien Shan (Kazakhstan/Kyrgyzstan) using remote sensing data. *Glob Planet Change*. 56:1–12. doi:10.1016/j.gloplacha.2006.07.009.

Bolch T, Buchroithner M, Pieczonka T. 2008. Planimetric and volumetric glacier changes in the Khumbu Himal, Nepal, since 1962 using Corona, Landsat TM and ASTER data. *J Glaciol*. 54:592–600.
Bolch T, Kulkarni A, Kääb A, Huggel C, Paul F, Cogley JG, Frey H, Kargel JS, Fujita K, Scheel M, et al. 2012. The state and fate of Himalayan glaciers. *Science*. 336:310–314. doi:10.1126/science.1215828.
Bolch T, Menounos B, Wheate R. 2010. Landsat-based inventory of glaciers in Western Canada, 1985–2005. *Remote Sens Environ*. 114:127–137. doi:10.1016/j.rse.2009.08.015.
Brown LE, Hannah DM, Milner AM. 2007. Vulnerability of alpine stream biodiversity to shrinking glaciers and snowpacks. *Glob Chang Biol*. 13:958–966. doi:10.1111/j.1365-2486.2007.01341.x.
Chand P, Sharma MC. 2015. Glacier changes in the Ravi basin, North-Western Himalaya (India) during the last four decades (1971-2010/13). *Glob Planet Change*. 135:133–147. doi:10.1016/j.gloplacha.2015.10.013.
DeBeer CM, Sharp MJ. 2007. Recent changes in glacier area and volume within the Southern Canadian Cordillera. *Ann Glaciol*. 46:215–221. doi:10.3189/172756407782871710.
Devjatkin EV. 1981. Cenozoic of inner Asia. Moscow: Nauka, 196 pp (In Russian).
Earl L, Garnder A. 2016. A satellite-derived glacier inventory for North Asia. *Ann Glaciol*. 57:50–60. doi:10.3189/2016AoG71A008.
Enkhtaivan D. 2006. Physical-geographical characteristics of the Altai region. In: Vogtmann H, Dobrestov N, editors. Environmental security and sustainable land use: with special reference to Central Asia. Dordrecht: Springer; p. 349–351.
Francou B, Vuille M, Wagnon P, Mendoza J, Sicart J-E. 2003. Tropical climate change recorded by a glacier in the central Andes during the last decades of the twentieth century: Chacaltaya, Bolivia, 16°S. *J Geophys Res*. 108:4154. doi:10.1029/2002JD002959.
Frey H, Paul F. 2012. On the suitability of the SRTM DEM and ASTER GDEM for the compilation of topographic parameters in glacier inventories. *Int J Appl Earth Obs Geoinf*. 18:480–490. doi:10.1016/j.jag.2011.09.020.
Frey H, Paul F, Strozzi T. 2012. Compilation of a glacier inventory for the Western Himalayas from satellite data: methods, challenges, and results. *Remote Sens Environ*. 124:832–843. doi:10.1016/j.rse.2012.06.020.
Ganiushkin D, Chistyakov K, Kunaeva E. 2015. Fluctuation of glaciers in the southeast Russian Altai and northwest Mongolia mountains since the Little Ice Age maximum. *Environ Earth Sci*. 74:1883–1904. doi:10.1007/s12665-015-4301-2.
Gardent M, Rabatel A, Dedieu J, Deline P. 2014. Multitemporal glacier inventory of the French Alps from the late 1960s to the late 2000s. *Glob Planet Change*. 120:24–37. doi:10.1016/j.gloplacha.2014.05.004.
Granshaw FD, Fountain AG. 2006. Glacier change (1958–1998) in the north cascades National Park complex, Washington, USA. *J Glaciol*. 52:251–256.
Grunert J, Lehmkuhl F, Walther M. 2000. Paleoclimatic evolution of the Uvs Nuur basin and adjacent areas (Western Mongolia). *Quat Int*. 65–66:171–192. doi:10.1016/S1040-6182(99)00043-9.
Herren PA, Eichler A, Machguth H, Papina T, Tobler L, Zapf A, Schwikowski M. 2013. The onset of neoglaciation 6000 years ago in western Mongolia revealed by an ice core from the Tsambagarav mountain range. *Quat Sci Rev*. 69:59–68. doi:10.1016/j.quascirev.2013.02.025.
Hodson A, Anesio AM, Tranter M, Fountain A, Osborn M, Priscu J, Laybourn-Parry J, Sattler B. 2008. Glacial Ecosystems. *Ecol Monogr*. 78:41–67.
IPCC. 2013. Climate change 2013: The physical science basis. Contribution of working group I to the fifth assessment report of the Intergovernmental panel on climate change. Stocker TF, Qin D, Plattner G-K, Tignor M, Allen SK, Boschung J, Nauels A, Xia Y, Bex V, Midgley PM, editors. Cambridge: Cambridge University Press. 1535 pp. doi:10.1017/CBO9781107415324.
Kääb A, Winsvold S, Altena B, Nuth C, Nagler T, Wuite J. 2016. Glacier remote sensing using sentinel-2. Part I: radiometric and geometric performance, and application to ice velocity. *Remote Sens*. 8:598. doi:10.3390/rs8070598.
Kadota T, Gombo D. 2007. Recent glacier variations in Mongolia. *Ann Glaciol*. 46:185–188.
Kadota T, Gombo D, Kalsan P, Namgur D. 2011. Glaciological research in the Mongolian Altai, 2003–2009. *Bull Glaciol Res*. 29:41–50.
Kamp U, McManigal KG, Dashtseren A, Walther M. 2013. Documenting glacial changes between 1910, 1970, 1992 and 2010 in the Turgen Mountains, Mongolian Altai, using repeat photographs, topographic maps, and satellite imagery. *Geogr J*. 179:248–263. doi:10.1111/j.1475-4959.2012.00486.x.
Kamp U, Pan CG. 2015. Inventory of glaciers in Mongolia, derived from Landsat imagery from 1989 to 2011. *Geogr Ann Ser A Phys Geogr*. 97:653–669. doi:10.1111/geoa.12105.
Kargel JS, Abrams MJ, Bishop MP, Bush A, Hamilton G, Jiskoot H, Kääb A, Kieffer HH, Lee EM, Paul F, et al. 2005. Multispectral imaging contributions to global land ice measurements from space. *Remote Sens Environ*. 99:187–219. doi:10.1016/j.rse.2005.07.004.
Klinge M. 2001. Glacial-geomorphologic investigations in the Mongolian Altai: a contribution to the late quaternary landscape and climate history of western Mongolia. Aachen: Aachener Geographische Arbeiten, 35, 125 pp (In German).
Khromova T, Nosenko G, Kutuzov S, Muraviev A, Chernova L. 2010. Glacier area changes in Northern Eurasia. *Environ Res Lett*. 9:1–11. doi:10.1088/1748-9326/9/1/015003.

Khrustsky VS, Golubeva EI. 2008. Dynamics of the glaciers of the Turgen-Kharkhira mountain range (western Mongolia). *Geogr Nat Resour*. 29:278–287.
Krumwiede BS, Kamp U, Leonard GJ, Kargel S, Dashtseren A, Walther M. 2014. Recent glacier changes in the Mongolian Altai Mountains: Case studies from Munkh Khairkhan and Tavan Bogd 2.
Lehmkuhl F. 1999. Rezente und jungpleistozäne Formungs- und Prozeßregionen im Turgen-Kharkhiraa, Mongolischer Altai. *Die Erde* 130:151–172.
Lutz F, Immerzeel WW, Shrestha B, Bierkens MFP. 2014. Consistent increase in high Asia's runoff due to increasing glacier melt and precipitation. *Nat Clim Chang*. 4:587–592. doi:10.1038/nclimate2237.
Lynch CM, Barr ID, Mullan D, Ruffell A. 2016. Rapid glacial retreat on the Kamchatka Peninsula during the early 21st century. *Cryosphere*. 10:1809–1821. doi:10.5194/tc-10-1809-2016.
Muhlfeld CC, Giersch JJ, Hauer FR, Pederson GT, Luikart G, Peterson DP, Downs CC, Fagre DB. 2011. Climate change links fate of glaciers and an endemic alpine invertebrate. *Clim Change*. 106:337–345. doi:10.1007/s10584-011-0057-1.
Nuimura T, Sakai A, Taniguchi K, Nagai H, Lamsal D, Tsutaki S, Kozawa A, Hoshina Y, Takenaka S, Omiya S, Tsunematsu K, Tshering P, Fujita K. 2015. The GAMDAM glacier inventory: a quality-controlled inventory of Asian glaciers. *Cryosphere* 9:849–864. doi:10.5194/tc-9-849-2015.
Nuth C, Kohler J, König M, Von Deschwanden A, Hagen JO, Kääb A, Moholdt G, Pettersson R. 2013. Decadal changes from a multi-temporal glacier inventory of Svalbard. *Cryosphere*. 7:1603–1621. doi:10.5194/tc-7-1603-2013.
Oerlemans J. 2005. Extracting a climate Signla from 169 glacier records. *Science*. 308:675–677. doi:10.1126/science.1107046.
Osipov EY, Osipova OP. 2014. Mountain glaciers of southeast Siberia : current state and changes since the Little Ice Age. *Ann Glaciol*. 55:167–176. doi:10.3189/2014AoG66A135.
Osmonov A, Bolch T, Xi C, Kurban A, Guo W. 2013. Glacier characteristics and changes in the Sary-Jaz River Basin (Central Tien Shan, Kyrgyzstan) – 1990–2010. *Remote Sens Lett*. 4:725–734. doi:10.1080/2150704X.2013.789146.
Paul F, Barrand NE, Baumann S, Berthier E, Bolch T, Casey K, Nosenko G, Frey H, Joshi SP, Konovalov V, et al. 2013. On the accuracy of glacier outlines derived from remote-sensing data. *Ann Glaciol*. 54:171–182. doi:10.3189/2013AoG63A296.
Paul F, Kääb A, Haeberli W. 2007. Recent glacier changes in the Alps observed by satellite : consequences for future monitoring strategies. *Glob Planet Change*. 56:111–122. doi:10.1016/j.gloplacha.2006.07.007.
Paul F, Mölg N. 2014. Hasty retreat of glaciers in northern Patagonia from 1985 to 2011. *J Glaciol*. 60:1033–1043. doi:10.3189/2014JoG14J104.
Paul F, Winsvold S, Kääb A, Nagler T, Schwaizer G. 2016. Glacier remote sensing using sentinel-2. Part II: mapping glacier extents and surface facies, and comparison to Landsat 8. *Remote Sens*. 8:575. doi:10.3390/rs8070575.
Pope A, Rees WG, Fox AJ, Fleming A. 2014. Open access data in polar and cryospheric remote sensing 6183–6220. doi:10.3390/rs6076183
Racoviteanu AE, Arnaud Y, Williams MW, Manley WF. 2015. Spatial patterns in glacier characteristics and area changes from 1962 to 2006 in the Kanchenjunga-Sikkim area, Eastern Himalaya. *Cryosphere*. 9:505–523. doi:10.5194/tc-9-505-2015.
Racoviteanu AE, Paul F, Raup B, Khalsa SJS, Armstrong R. 2009. Challenges and recommendations in mapping of glacier parameters from space: results of the 2008 global land ice measurements from space (GLIMS) workshop, Boulder, Colorado, USA. *Ann Glaciol*. 50:53–69. doi:10.3189/172756410790595804.
Raup B, Kääb A, Kargel JS, Bishop MP, Hamilton G, Lee E, Paul F, Rau F, Soltesz D, Khalsa SJS, et al. 2007. Remote sensing and GIS technology in the global land Ice measurements from space (GLIMS) project. *Comput Geosci*. 33:104–125. doi:10.1016/j.cageo.2006.05.015.
Roy DP, Wulder MA, Loveland TR, Woodcock CE, Allen RG, Anderson MC, Helder D, Irons JR, Johnson DM, Kennedy R, et al. 2014. Landsat-8: science and product vision for terrestrial global change research. *Remote Sens Environ*. 145:154–172. doi:10.1016/j.rse.2014.02.001.
Selivanov EI. 1972. Neotectonics and geomorphology of the Mongolian people's republic. Nedra: State Publishing House, 293 pp (In Russian).
Shahgedanova M, Nosenko G, Khromova T, Muraveyev A. 2010. Glacier shrinkage and climatic change in the Russian Altai from the mid - 20th century : An assessment using remote sensing and PRECIS regional climate model. *J Geophys Res*. 115:1–12. doi:10.1029/2009JD012976.
Shinneman LC, Umbanhowar CE, Edlund MB, Soninkhishig N. 2010. Late-Holocene moisture balance inferred from diatom and lake sediment records in Western Mongolia. *Holocene*. 20:123–138. doi:10.1177/0959683609348861.
Stokes CR, Shahgedanova M, Evans IS, Popovnin VV. 2013. Accelerated loss of alpine glaciers in the Kodar Mountains, south-eastern Siberia. *Glob Planet Change*. 101:82–96. doi:10.1016/j.gloplacha.2012.12.010.
Surazakov B, Aizen VB, Aizen EM, Nikitin SA. 2007. Glacier changes in the Siberian Altai Mountains, Ob river basin, (1952–2006) estimated with high resolution imagery. *Environ Res Lett*. 2:45017. doi:10.1088/1748-9326/2/4/045017.
Syromyatina MV, Kurochkin YN, Bliakharskii DP, Chistyakov KV. 2015. Current dynamics of glaciers in the Tavan Bogd Mountains (Northwest Mongolia). *Environ Earth Sci*. 74:1905–1914. doi:10.1007/s12665-015-4606-1.

Tennant C, Menounos B, Wheate R, Clague JJ. 2012. Area change of glaciers in the Canadian Rocky Mountains, 1919 to 2006. *Cryosphere*. 6:1541–1552. doi:10.5194/tc-6-1541-2012.

Tielidze L. 2016. Glaciers change over the last century, Caucasus mountains, Georgia, observed by the old topographical maps, landsat and ASTER satellite imagery. *Cryosphere*. 10:713–725. doi:10.5194/tcd-9-3777-2015.

Tsutomu K, Gombo D. 2007. Recent glacier variations in Mongolia. *Ann Glaciol*. 46:185–188.

Walther M, Dashtseren A, Kamp U, Temujin K, Meixner F, Pan CG, Gansukh Y. 2017. Glaciers, permafrost and lake levels at the Tsengel Khairkhan mass, Mongolian Altai, during the late Pleistocene and Holocene. *Geosci (Basel)*. 7. doi:10.3390/geosciences7030073.

Winsvold S, Kääb A, Nuth C. 2016. Regional glacier mapping using optical satellite data time series. *IEEE J Sel Top Appl Earth Obs Remote Sens*. 9:3698–3711. doi:10.1109/JSTARS.2016.2527063.

Wulder MA, Masek JG, Cohen WB, Loveland TR, Woodcock CE. 2012. Remote sensing of environment opening the archive: how free data has enabled the science and monitoring promise of Landsat. *Remote Sens Environ*. 122:2–10. doi:10.1016/j.rse.2012.01.010.

Yabouki H, Ohata T. 2009. The recent glacier changes in the Mongolian Altai Mountains. EOS (Transactions, American Geophysical Union), 90: Fall Meeting Supplement, Abstract #C31C- 0454.

Zemp M, Frey H, Gärtner-Roer I, Nussbaumer SU, Hoelzle M, Paul F, Haeberli W, Denzinger F, Ahlstrøm AP, Anderson B, et al. 2015. Historically unprecedented global glacier decline in the early 21st century. *J Glaciol*. 61:745–762. doi:10.3189/2015JoG15J017.

Zhang Y, Enomoto H, Ohata T, Kitabata H, Kadota T, Hirabayashi Y. 2016. Projections of glacier change in the Altai mountains under twenty-first century climate scenarios. *Clim Dyn*. doi:10.1007/s00382-016-3006-x.